



Amphiphilic multi-charged cyclodextrins and vitamin K co-assembly as a synergistic coagulant†

Pei-yu Li, Yong Chen, Chang-hui Chen and Yu Liu *

Cite this: *Chem. Commun.*, 2019, 55, 11790

Received 24th August 2019,
Accepted 2nd September 2019

DOI: 10.1039/c9cc06545h

rsc.li/chemcomm

Balancing and neutralizing heparin dosing after surgeries and hemodialysis treatment is of great importance in medical and clinical fields. In this study, a series of new amphiphilic multi-charged cyclodextrins (AMCD)s as anti-heparin coagulants were designed and synthesized. The AMCD assembly was capable of selective heparin binding through multivalent bonding and showed a better neutralizing effect towards both unfractionated heparin and low molecular weight heparin than protamine in plasma. Meanwhile, an AMCD and vitamin K (VK) co-assembly was prepared to realize heparin-responsive VK release and provide a novel VK deficiency treatment for hemodialysis patients. This AMCD–VK co-assembly for heparin neutralization & vitamin K supplementation synergistic coagulation represents a promising candidate as a clinical anti-heparin coagulant.

Heparin is a widely used anticoagulant in clinics which can bind to anti thrombin III and cause the inactivation of factor Xa. UFH is used to maintain blood fluidity during hemodialysis.^{1,2} LMWH and fondaparinux are applied for the treatment of deep vein thrombosis and pulmonary embolism.^{3,4} To balance and neutralize heparin dosing, protamine is used as a heparin inhibitor which can neutralize heparins by forming – with varying degrees of success – inert complexes.⁵ However, the clinical use of protamine has several medical risks like hypotension and serious allergic reactions caused by immune responses to this exogenous protein.^{6,7} Until now, protamine has no approved medicinal substitute and its production is limited by the wild and bred livestock availability. Meanwhile, protamine is only partially active against LMWHs and has almost no effect towards fondaparinux, both of which are widely used in the clinic.⁸ Thus, the search for alternatives to protamine has gained extensive attention and lots of candidates have been reported including small molecules,⁹

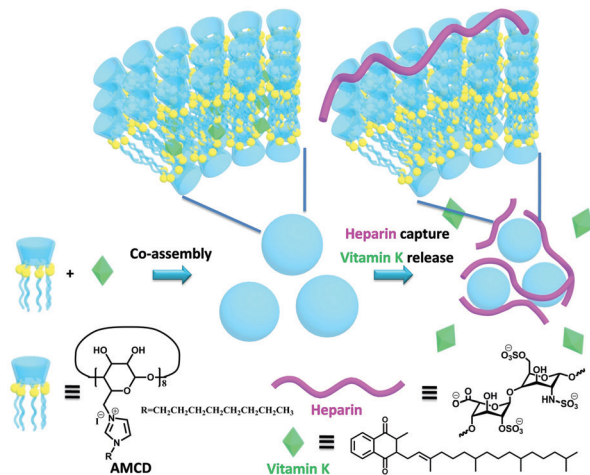
proteins and peptides,^{10–12} linear and branched polymers,^{13–15} and macrocycles.^{16,17} Furthermore, a significant proportion of hemodialysis patients have a functional vitamin K deficiency with the risk of modifiable biological effects.¹⁸ Vitamin K supplementation after hemodialysis and surgery is also a noteworthy problem.¹⁹

Supramolecular assembly based on macrocycles has gained lots of interest as a functional bio-sensing, drug delivery and disease treatment platform.^{20–27} Multivalent co-assembly based on amphiphilic macrocycles could provide high specificity and selectivity towards bioactive molecules.²⁸ To neutralize heparin and supplement VK delivery at the same time, we plan to construct a new coagulant strategy based on amphiphilic supramolecular assembly with multivalent binding sites on the surface and drug delivery in the hydrophobic inner layer.

Herein, we wish to report a novel anti-heparin coagulant based on amphiphilic multi-charged cyclodextrin (AMCD) assembly as shown in Scheme 1. A series of novel amphiphilic cyclodextrins were synthesized with modification of positively charged imidazolium cation groups and alkyl chains at the lower rim. Due to the amphiphilic nature, these AMCDs could self-assemble and co-assemble with hydrophobic drugs in aqueous media. The imidazolium cation groups together with the cyclodextrin cavity at the surface of the AMCD assembly could strongly capture heparin through synergic multivalent binding. The high binding affinity towards heparin was measured by an indicator displacement assay (IDA) in which 8-hydroxypyrene-1,3,6-trisulfonic acid trisodium salt (HPTS) was chosen as the indicator. The host–guest complex of AMCD–HPTS could also be used as a reporting pair to monitor heparin concentration by fluorescence. Activated partial thromboplastin time (aPTT) experiments confirmed that AMCDs could effectively neutralize heparin in plasma and one of the AMCDs, AMCD-8cγ showed better anti-heparin ability than protamine towards UFH and LMWH. Furthermore, the AMCD could co-assemble with VK and the assembly was characterized by TEM and DLS experiments. A morphology transformation from spherical particles to square particles was also observed after the capture of heparin by TEM images. Meanwhile, along with the morphology

College of Chemistry, State Key Laboratory of Elemento-Organic Chemistry, Nankai University, Tianjin 300071, P. R. China. E-mail: yuliu@nankai.edu.cn

† Electronic supplementary information (ESI) available: Detailed synthesis, characterization data, Job's plots, dynamic light scattering, zeta potential and transmission electron microscopy images. See DOI: 10.1039/c9cc06545h



Scheme 1 Systematic presentation of the construction of AMCD–VK co-assembly, the heparin capture & vitamin K release process and the corresponding molecular structures of AMCD and VK.

transformation, VK was released from the AMCD assembly. The capture of heparin by AMCD assembly together with the release of VK would provide a novel synergistic coagulant treatment. We believe that this AMCD–VK co-assembly will become a novel heparin neutralization & vitamin K supplementation synergistic coagulant strategy and have potential application value in clinical surgery.

Heparin is a co-polymer composed of glucosamine, L-aldoside, N-acetylglucosamine, and D-glucuronic acid and is a typical negatively charged polysaccharide. Referring to the structural features of heparin, we designed the artificial receptor AMCD as a promising anti-heparin coagulant with the following considerations. First, cyclodextrin were employed as the non-synthetic macrocyclic scaffold benefiting from their inexpensive preparation and facial modification. Second, positively charged imidazolium cation groups at the lower rim of AMCD could provide electrostatic interaction binding sites towards the sulfonic acid group and carboxylic acid group of heparin. Third, the cavities of cyclodextrins and the hydroxyl groups on the upper rim possessed similar nature to the glucose units of heparin which further enhanced the binding affinities through hydrophobic interaction and hydrogen bonds. Finally and most importantly, the AMCD assembly provided multiple binding sites on the surface towards the heparin macromolecular chain which would greatly promote the neutralization of heparin. Collectively, based on these considerations, AMCD was designed as an artificial heparin inhibitor which was expected to show strong binding affinity towards heparin *via* multivalent and synergistic effects of electrostatic, hydrogen bond and hydrophobic interactions. The AMCD was synthesized by dissolving Octakis (6-deoxy-6-iodo)- γ -cyclodextrin in 1-octylimidazole and stirred at 80 °C under an argon atmosphere for 2 days. ¹H NMR, ¹³C NMR and mass spectra were used to characterize the AMCDs as provided in the ESI[†] (Fig. S1–S4).

Next, the binding behaviour between AMCD and heparin was studied. The NMR experiment was first carried out as shown in the ESI[†] (Fig. S9 for AMCD–UFH complex and Fig. S10 for

AMCD–LMWH respectively). Since heparin is a polymer with a large molecular weight, only broadening resonance peaks were observed which disappeared after the addition of AMCD. The reason was that the protons of heparin were located within the cavity of AMCD and shielded by the cyclic structure by forming an inclusion complex between heparin and AMCD. Since, the AMCD host is amphiphilic and tends to form an assembly, calorimetric titration was therefore ruled out because the heat change caused by the assembly process could disturb the measurement of binding affinity. As an alternative approach, fluorescent IDA was chosen to study the binding behaviour between AMCD and heparin. IDA, the use of synthetic receptors with competitive binding assays, has been popularized as a standard strategy for molecular sensing, complementary to the approach of direct sensing. We employed IDA to not only determine the binding affinity between AMCD and heparin, but also to concurrently offer the opportunity for fluorescence sensing of heparin concentration. HPTS was screened as the optimal reporter dye, owing to its high brightness, strong binding with AMCD and drastic complexation-induced enhancement of fluorescence (Fig. S5, ESI[†]). The binding stoichiometry between AMCD and HPTS was determined to be 1:1 according to the Job's plot (Fig. S6, ESI[†]). The association constant (K_a), extracted from the fluorescence titration, was fitted as $(5.0 \pm 0.2) \times 10^6 \text{ M}^{-1}$. The AMCD–HPTS complex was also characterized by ¹H NMR and rotating frame Overhauser enhancement spectroscopy (ROESY) (Fig. S7 and S8, ESI[†]). The displacement of AMCD–HPTS by gradual addition of UFH resulted in reduction of HPTS fluorescence (Fig. 1a). The data were well fitted by a 1:1 competitive binding model, giving a K_a value of $(2.4 \pm 0.1) \times 10^6 \text{ M}^{-1}$. To validate the synergistic effect of several interactions on binding between AMCD and heparin, we further tested changes in the fluorescence intensity of AMCD–HPTS caused by other important negatively charged polysaccharides such as LMWH, hyaluronic acid (HYA) and alginic acid (ALG). As shown in Fig. 1c (Fig. S11–S13, ESI[†]), the addition of LMW heparin to the AMCD–HPTS caused

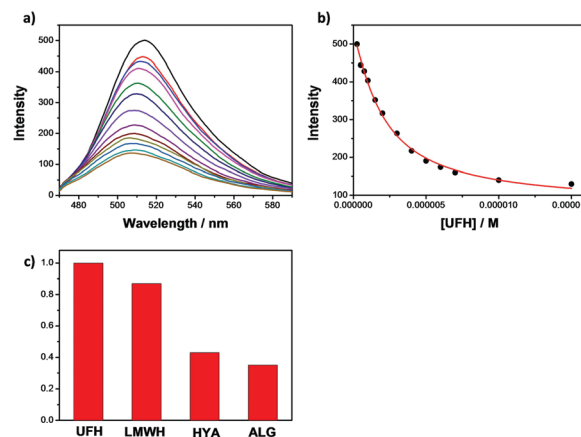


Fig. 1 (a) Competitive titration of AMCD–HPTS (1/1 μM) with UFH (up to 15 μM). (b) The associated titration curve at $\lambda_{em} = 515 \text{ nm}$ and the fit according to a 1:1 competitive binding mode. (c) The binding affinities of AMCD towards UFH, LMWH, hyaluronic acid (HA) and alginic acid (ALG). All the experiments were carried out in 10 mM tris-HCl buffer pH = 7.4.

89% signal change as UFH while the addition of HYA and ALG only caused 41% and 38% respectively. The addition of other neutral or positively charged polysaccharide caused almost no change of AMCD–HPTS fluorescence. These results proved the high selectivity of AMCD towards UFH and LMWH due to the synergistic effect of multiple sites and multiple non-covalent interactions.

Next, we further study the properties of AMCD assembly and the AMCD–heparin co-assembly. Transmission electron microscopy (TEM), dynamic light scattering (DLS) and zeta potential experiments were employed to identify the morphology, size and surface potential of the assembly. As shown in Fig. 2, uniform spherical particles could be observed in the TEM image of the AMCD assembly while square particles were found in the TEM image of the AMCD–heparin co-assembly. In DLS measurements, particles formed by AMCD assembly exhibited a narrow size distribution with a hydrodynamic radius (R_h) of 227 nm at a scattering angle of 90° while the particles formed by AMCD–heparin co-assembly possessed a R_h of 88 nm. The reduction of particles size found by the DLS experiment was in nice agreement with the TEM results. Meanwhile, the zeta potential of AMCD assembly was measured as +42 mV while the zeta potential of AMCD–heparin co-assembly was +22 mV. The positive zeta potential of AMCD self-assembly was due to the positively charged imidazolium cation groups at the upper of AMCD. The reduction of zeta potential to the AMCD–heparin co-assembly was in accordance with the addition of negatively charged heparin with sulfonic acid and carboxylic acid groups. The TEM image of heparin (Fig. S17, ESI[†]) as a control also showed discriminative morphology compared with the AMCD assembly and AMCD–heparin co-assembly. Combining all the

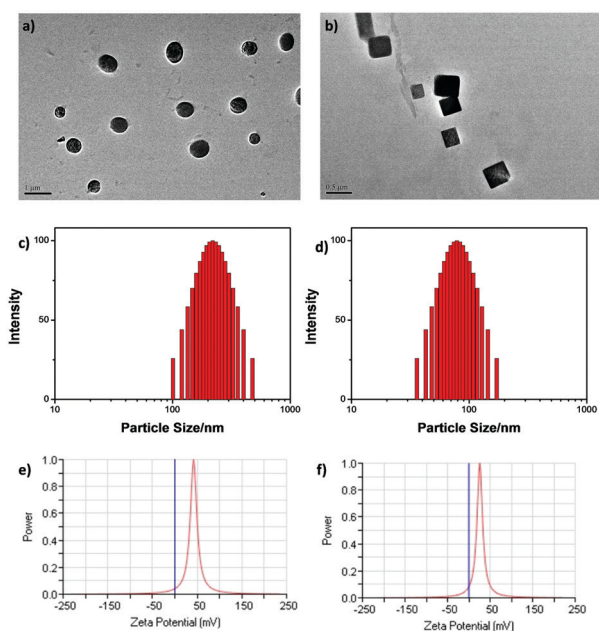


Fig. 2 The TEM images of (a) the AMCD assembly and (b) the co-assembly. The DLS data of (c) AMCD and (d) the AMCD–heparin co-assembly. The zeta potential of (e) AMCD and (f) the AMCD–heparin co-assembly.

forementioned results, we concluded that with the capture of heparin through multivalent binding, the AMCD assembly became smaller and transformed into a novel morphology.

The heparin neutralization ability of the AMCDs was studied by aPTT clotting assays in plasma. The aPTT measurement was the primary laboratory test used to monitor and adjust UFH. The performances of four AMCDs (4c β , 8c β , 4c γ and 8c γ) and protamine (as reference) as antidotes for clinically used UFH were investigated. As shown in Fig. 3, the 8c β and 8c γ had better neutralization efficiency towards UFH in plasma than 4c β , 4c γ and protamine. This was because 8c β and 8c γ possessed longer alkyl chains and more easily form assembly to realize a multivalent binding towards UFH. Meanwhile, 8c γ showed better neutralization ability than 8c β which we believe was caused by the higher number of positive charges. The neutralization towards LMWH was also studied as shown in Fig. S14 (ESI[†]). More interestingly, we found that both the 4c γ and 8c γ showed better LMWH neutralization ability than protamine. With the increasing of antidote concentration from 10 to 20 $\mu\text{g mL}^{-1}$, the aPTT of protamine changed slightly while the aPTT of 4c γ and 8c γ kept reducing. Protamine is unable to completely reverse the anticoagulant effect of LMWH which limited its clinical use while UFH may cause platelet aggregation and bleeding complications. For these reasons, we believe that with the utilization of a better antidote such as AMCD–8c γ , the application of LMWH could be broadened.

The capability of AMCD assembly on loading coagulant drugs was examined by using VK, also known as coagulation vitamin. Vitamin K is a cofactor for γ -glutamyl carboxylase, the enzyme responsible for the formation of matrix γ -carboxyglutamate residues that confer calcium-binding properties to a small class of proteins, referred to as vitamin K-dependent proteins including coagulation factors II, VII, IX, and X. A significant proportion of hemodialysis patients have a functional vitamin K deficiency and may be at greater risk of potentially modifiable biological effects. We wish to construct a VK carrier with AMCD to solve the vitamin K deficiency of hemodialysis patients during the heparin neutralization process. As shown in Fig. 4a, the calibration curve line of VK was measured by UV-vis absorption spectra of different concentrations of VK in water (Fig. S15, ESI[†]). As observed from the calibration curve line, the absorption of VK at 330 nm was in a linear relationship with the VK concentration in the range of 2–22.5 μM . An AMCD and VK co-assembly (AMCD–VK) was prepared through the method in the supplementary information. Since the AMCD has no absorption at 330 nm, from the UV-vis spectrum

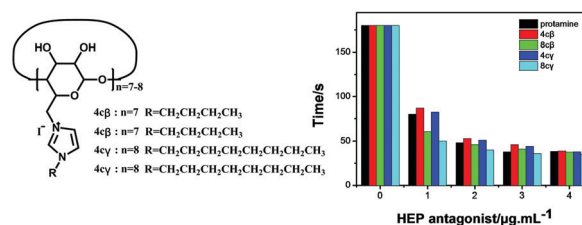


Fig. 3 aPTT clotting assay of UFH (0.3 USP mL^{-1}) plasma after addition of antagonist AMCDs (4c β , 8c β , 4c γ and 8c γ) or protamine sulfate as a reference.

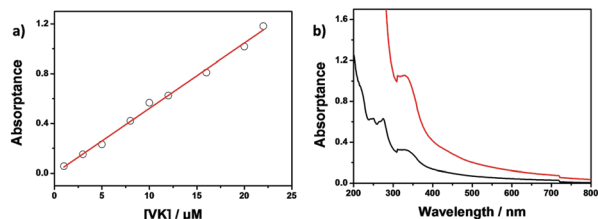


Fig. 4 (a) The UV-vis absorption calibration curve line of vitamin K at 330 nm. (b) The UV-vis absorption spectra of vitamin K loaded by AMCD self-assembly before (red line) and after (black line) the addition of heparin.

absorption of the AMCD-VK co-assembly (Fig. 4b), the concentration of VK could be calculated according to calibration curve line. The VK loading efficiency and the encapsulation efficiency were calculated as 6% and 40%, respectively. As the morphology transformation occurred after the capture of heparin which was observed by TEM and DLS, about 64% VK was released as calculated from the UV-vis absorption spectrum according to the calibration curve line of VK. The TEM image of AMCD-VK co-assembly was also presented in Fig. S16 (ESI[†]) as a control which showed no obvious difference compared with AMCD assembly. We believe that this AMCD-VK co-assembly strategy would provide heparin neutralization & vitamin K supplementation synergistic coagulation.

A series of novel amphiphilic multi-charged cyclodextrins was synthesized and AMCD-assembly was utilized for selective heparin binding. High binding affinity towards heparin was characterized by the IDA method and the sensing of heparin through fluorescence competitive binding was also achieved. The aPTT experiments also confirmed the highly efficient heparin neutralization by AMCD in plasma and one of the AMCDs 8cγ showed a high neutralization effect towards not only UFH but also LMWH which proved to be a better protamine alternative. More interestingly, the transformation of the AMCD assembly after the capture of heparin could realize heparin-stimuli responsive release of vitamin K. This AMCD-VK co-assembly strategy would provide a heparin neutralization & vitamin K supplementation synergistic coagulation and have potential enlightenment in biochemistry, medical and clinical fields.

We thank NNSFC (21672113, 21772099, 21971127 and 21861132001) for financial support.

Conflicts of interest

There are no conflicts to declare.

Notes and references

- N. Mackman, *Nature*, 2008, **451**, 914.
- H. Bussey and J. L. Francis, *Pharmacotherapy*, 2004, **24**, 103S.
- J. I. Weitz, *N. Engl. J. Med.*, 1997, **337**, 688.
- M. Suranyi and J. S. Chow, *Nephrology*, 2010, **15**, 386.
- S. M. Bromfield, E. Wilde and D. K. Smith, *Chem. Soc. Rev.*, 2013, **42**, 9184.
- S. Wan, J.-L. LeClerc and J.-L. Vincent, *Chest*, 1997, **112**, 676–692.
- J. W. Vandiver and T. G. Vondracek, *Pharmacotherapy*, 2012, **32**, 546–558.
- I. Melnikova, *Nat. Rev. Drug Discovery*, 2009, **8**, 353.
- M. Schuksz, M. M. Fuster, J. R. Brown, B. E. Crawford, D. P. Ditto, R. Lawrence, C. A. Glass, L. Wang, Y. Tor and J. D. Esko, *Proc. Natl. Acad. Sci. U. S. A.*, 2008, **105**, 13075.
- R. Godavarti and R. Sasisekharan, *J. Biol. Chem.*, 1998, **273**, 248.
- T. Ammar and C. F. Fisher, *Anesthesiology*, 1997, **86**, 1382.
- H. Wu, R. Lundblad and F. Church, *Blood*, 1995, **85**, 421.
- M. T. Kalathottukaren, S. Abbina, K. Yu, R. A. Shenoi, A. L. Creagh, C. Haynes and J. N. Kizhakkedathu, *Biomacromolecules*, 2017, **18**, 3343.
- J. Wen, M. Weinhart, B. Lai, J. Kizhakkedathu and D. E. Brooks, *Biomaterials*, 2016, **86**, 42.
- S. Välimäki, A. Khakalo, A. Ora, L. S. Johansson, O. J. Rojas and M. A. Kostianen, *Biomacromolecules*, 2016, **17**, 2891.
- T. Mecca, G. M. L. Consoli, C. Geraci, R. L. Spina and F. Cunsolo, *Org. Biomol. Chem.*, 2006, **4**, 3763.
- M. T. Välimäki, N. K. Beyeh, V. Linko, R. H. Ras and M. A. Kostianen, *Nanoscale*, 2018, **10**, 14022.
- R. M. Pilkey, A. R. Morton, M. B. Boffa, C. Noordhof, A. G. Day, Y. Su, L. M. Miller, M. L. Koschinsky and S. L. Booth, *Am. J. Kidney Dis.*, 2007, **49**, 432–439.
- R. Westenfeld, T. Krueger, G. Schlieper, E. C. M. Cranenburg, E. J. Magdeleyns, S. Heidenreich, S. Holzmann, C. Vermeer, W. Jahn-Dechent, M. Ketteler, J. Floege and L. J. Schurgers, *Am. J. Kidney Dis.*, 2012, **59**, 186–195.
- P. Li, Y. Chen and Y. Liu, *Chin. Chem. Lett.*, 2019, **30**, 1190–1197.
- H. Zhu, L. Shangguan, B. Shi, G. Yu and F. Huang, *Mater. Chem. Front.*, 2018, **2**, 2152–2174.
- X. Liu, J. Zhang, M. Fadeev, Z. Li, V. Wulf, H. Tian and I. Willner, *Chem. Sci.*, 2019, **10**, 1008–1016.
- G. Sun, Z. He, M. Hao, M. Zuo, Z. Xu, X. Y. Hu, J. J. Zhu and L. Wang, *J. Mater. Chem. B*, 2019, **7**, 3944–3949.
- X. S. Du, Q. Jia, C. Y. Wang, K. Meguellati and Y. W. Yang, *Chem. Commun.*, 2019, **55**, 5736–5739.
- S. Z. F. Phua, C. Xue, W. Q. Lim, G. Yang, H. Chen, Y. Zhang, C. F. Wijaya, Z. Luo and Y. Zhao, *Chem. Mater.*, 2019, **31**, 3349–3358.
- Y. Chen, F. Huang, Z. T. Li and Y. Liu, *Sci. China: Chem.*, 2018, **61**, 979–992.
- G. Yu, J. Zhou, J. Shen, G. Tang and F. Huang, *Chem. Sci.*, 2016, **7**, 4073–4078.
- Z. Xu, S. Jia, W. Wang, Z. Yuan, B. Jan Ravoo and D.-S. Guo, *Nat. Chem.*, 2019, **11**, 86–93.